

# The genomic arrangement of T cell receptor variable genes is a determinant of the developmental rearrangement pattern

Na Xiong, Jeanne E. Baker\*, Chulho Kang, and David H. Raulet<sup>†</sup>

Department of Molecular and Cell Biology and Cancer Research Laboratory, 489 Life Sciences Addition, University of California, Berkeley, CA 94720

Communicated by Martin G. Weigert, Princeton University, Princeton, NJ, June 17, 2003 (received for review September 27, 2002)

**Developmentally regulated V(D)J recombination profoundly influences immune repertoires, but the underlying mechanisms are poorly understood. In the endogenous T cell receptor C $\gamma$ 1 cluster, the 3' V $\gamma$ 3 gene (closest to J $\gamma$ 1) rearranges preferentially in the fetal period whereas rearrangement of the 5' V $\gamma$ 2 gene predominates in the adult. Reversing the positions of the V $\gamma$ 2 and V $\gamma$ 3 genes in a genomic transgene resulted in decreased rearrangement of the now 5' V $\gamma$ 3 gene in the fetal thymus and increased rearrangement of the now 3' V $\gamma$ 2 gene. The reversed rearrangement pattern was not accompanied by significant changes in chromatin accessibility of the relocated V $\gamma$  genes. The results support a model in which the 3' location is the key determinant of rearrangement in the fetus, after which there is a promoter-dependent inactivation of V $\gamma$ 3 rearrangement in favor of V $\gamma$ 2 rearrangement.**

Specific V genes in T cell receptor (TCR)  $\gamma$  (1), TCR $\delta$  (2), and IgH (3, 4) loci rearrange preferentially at different stages of ontogeny. The mechanisms that differentially regulate recombination of various V, D, and J gene segments are poorly understood. One model is that local transcriptional regulatory elements control the accessibility of corresponding recombination signal sequences (RSS) to the recombinase, thereby regulating the lineage and stage specificity of V(D)J recombination (5–9).

Another factor that may contribute to developmental regulation of gene rearrangement is the gene segment location on the chromosome. In IgH, TCR $\gamma$ , and TCR $\delta$  loci, V genes that rearrange early in ontogeny are typically relatively proximal to the D or J gene segments (3, 6, 10–13). However, the evidence to date that rearrangement frequency is determined by the V gene location is purely correlative.

TCR V $\gamma$  gene rearrangements are subject to a particularly striking degree of developmental regulation. The TCR C $\gamma$ 1 cluster in mice consists of four V $\gamma$  gene segments in the order (5' to 3') V $\gamma$ 5, -2, -4, and -3, all of which recombine primarily with a single downstream J gene segment, J $\gamma$ 1. In early fetal thymocytes [embryonic day (E) 15], nearly all J $\gamma$ 1 rearrangements consist of V $\gamma$ 3 and to a lesser extent V $\gamma$ 4 rearrangements (11, 12). In contrast, V $\gamma$ 2 and V $\gamma$ 5 rearrangements dominate in the adult thymus (6, 11).

The ontogenic pattern of V $\gamma$  gene rearrangement is important in establishing the unique distribution of specific subsets of  $\gamma\delta$  T cells in different tissues. Early fetal  $\gamma\delta$  cells harboring V $\gamma$ 3 rearrangements migrate to the skin where they represent essentially all of the resident T cells, called dendritic epidermal T cells (DECs) (14). On the other hand, V $\gamma$ 2<sup>+</sup> and V $\gamma$ 5<sup>+</sup>  $\gamma\delta$  T cells represent the majority of  $\gamma\delta$  T cells in the lymph nodes, spleen, and blood.

Several lines of evidence demonstrate that developmentally regulated V $\gamma$  gene segment recombination is an intrinsic genetically programmed process. The most direct experiment used  $\gamma$ B, a 39-kb genomic transgene containing most of the unrearranged TCR C $\gamma$ 1 cluster, in which each of the V $\gamma$  genes (V $\gamma$ 2, V $\gamma$ 4, and V $\gamma$ 3) contained a frame-shift mutation that prevents functional expression. The V $\gamma$  genes in the  $\gamma$ B transgene rearranged at the

appropriate stage in thymic development despite the fact that the rearrangements could not directly influence the fate of cells in which they occurred (9). In like fashion, a targeted TCR $\delta$  gene deletion, which abrogates the formation of TCR $\gamma\delta$  receptors, did not disrupt the normal developmental pattern of V $\gamma$  gene rearrangement (15). Earlier studies demonstrated that nonproductive V $\gamma$  gene rearrangements exhibit a similar rearrangement pattern as productively rearranged alleles in the same cells (16). The pattern of V $\gamma$  gene germ-line transcription correlates with the rearrangement pattern, suggesting a possible link between rearrangement and transcriptional regulatory cues in this system (6). Furthermore, the decreased rearrangement of the V $\gamma$ 3 gene in the later stages of development correlated well with progressive local deacetylation (17).

We previously reported that V $\gamma$  gene promoter elements play a key role in regulating the developmental stage specificity of V $\gamma$  gene rearrangement (9). Starting with the  $\gamma$ B transgene backbone, fragments containing the promoter regions of the V $\gamma$ 2 and V $\gamma$ 3 genes were reciprocally swapped to generate the  $\gamma$ B-Pr-Sw transgene (previously called the  $\gamma$ Sw transgene). The promoter exchange reversed the pattern of rearrangement of these V $\gamma$  genes in the adult thymus, suggesting that the V $\gamma$  gene usage pattern in the adult thymus is controlled by promoter sequences.

Surprisingly, the promoter swap did not alter the pattern of V $\gamma$  transgene rearrangements in fetal thymocytes or in V $\gamma$ 3<sup>+</sup> DEC cells, a population that is derived from early fetal V $\gamma$ 3<sup>+</sup> thymocytes. Apparently, a distinct form of regulation is responsible for selective V $\gamma$  gene rearrangement in early fetal thymocytes. Here, we demonstrate that the fetal, but not the adult, pattern of rearrangement is determined by the location of V $\gamma$  genes in the gene cluster. The results represent direct evidence that V gene location is a determinant of the rearrangement pattern.

## Methods

**Generation of Transgenic Mice.** The  $\gamma$ B and  $\gamma$ B-Pr-SW (formerly called  $\gamma$ SW) transgenic mice have been described (9). The  $\gamma$ B-Gn-Sw transgene is identical to the  $\gamma$ B transgene except that a 2.3-kb Spel-EcoRI fragment containing the entire V $\gamma$ 2 gene segment was exchanged with a 1.6-kb HindIII-EcoRI fragment containing the entire V $\gamma$ 3 gene segment. The transgene inserts were injected into fertilized (C57BL/6  $\times$  CBA/J)F<sub>2</sub> eggs. Transgenic founders were identified by PCR of genomic DNA (9) and backcrossed serially to CBA/J mice (National Cancer Institute, Bethesda). The mice used in the experiments had been backcrossed two to four times. Transgene copy number was determined by quantitative Southern blotting of tail genomic DNA.

Abbreviations: TCR, T cell receptor; RSS, recombination signal sequence; DEC, dendritic epidermal T cell; LM-PCR, linker-mediated PCR; En, embryonic day *n*.

\*Present address: Elan Pharmaceuticals, 800 Gateway Boulevard, South San Francisco, CA 94080.

<sup>†</sup>To whom correspondence should be addressed. E-mail: raulet@uclink4.berkeley.edu.

© 2003 by The National Academy of Sciences of the USA

**PCR Primers and Linkers.** L2, L4, L3, J1, V2-3'a, V3-3'a, V3-3'b, 5'tubulin, and 3'tubulin primers have been described (6, 18). Primers PSV $\gamma$ 2 and PSV $\gamma$ 3 have been also described (9) as have the BW linker and BW1 primer (19). The sequence of VG2I primer is: GCTTCGTCTTCTTCTCCAAGG.

**Semiquantitative PCR and RT-PCR.** CD4<sup>-</sup>CD8<sup>-</sup> thymocytes were prepared by magnetic sorting (20). DECJs were prepared as described (21). Genomic DNA and total RNA were prepared as described (9, 22). Semiquantitative analysis of rearrangement of the V $\gamma$ 2 and V $\gamma$ 3 genes was performed as described (9). The ratios of V $\gamma$ 2 (Tg)/V $\gamma$ 3 (Tg) transgene rearrangement levels displayed below each data set in Fig. 2 were based on the previous determination of a ratio of 1/8 in the  $\gamma$ B (3) sample, by comparison with cell lines (9). The ratios in the other DNA samples were calculated by comparing the observed level of rearrangements based on the titrations shown to that in the  $\gamma$ B (3) sample, normalizing based on the tubulin PCRs.

The semiquantitative RT-PCR assay for quantitation of germ-line V $\gamma$  transcripts was modified from a previously described method (6, 20). Comparable amounts of total cellular RNA were reverse transcribed with the V2-3'a primer (for V $\gamma$ 2) or the V3-3'a primer (for V $\gamma$ 3) by using SuperScript II RNase H<sup>-</sup> reverse transcriptase (GIBCO/BRL). Reverse transcription products were serially diluted and subjected to semiquantitative PCR in the presence of [ $\alpha$ -<sup>32</sup>P]dCTP. For amplifying V $\gamma$ 2 sequences, we used the L2 or PSV $\gamma$ 2 primers in conjunction with the VG2I primer. For V $\gamma$ 3, we used the L3 or PSV $\gamma$ 3 primers in conjunction with the V3-3'b primer. The PCR products were digested with *Nru*I (for V $\gamma$ 2) or *Eco*RI (for V $\gamma$ 3) and run on a 5% polyacrylamide gel, which was dried and exposed to an x-ray film and a PhosphorImager (Molecular Dynamics). A semiquantitative RT-PCR for tubulin was used to normalize the samples.

**Detecting RSS Breaks Flanking V $\gamma$ 2 and V $\gamma$ 3 by Linker-Mediated PCR (LM-PCR).** RSS breaks flanking V $\gamma$ 2 and V $\gamma$ 3 were measured by LM-PCR, as described, with minor modifications (19). Briefly, thymic genomic DNA was ligated with a BW linker, serially diluted, and subjected to radioactive semiquantitative PCR with the BW1 and V $\gamma$ 2-3'a primers to detect V $\gamma$ 2 breaks, or with the BW1 and V $\gamma$ 3-3'b primers to detect V $\gamma$ 3 breaks. Semiquantitative PCR for tubulin was used to normalize the samples.

**Restriction Enzyme Accessibility Assay.** The assay was performed as described (23). Briefly, nuclei were prepared from E15 total thymocytes or adult CD4<sup>-</sup>CD8<sup>-</sup> thymocytes by Nonidet P-40 lysis and resuspended in suitable buffers supplemented with restriction enzymes (*Asp*-718 for V $\gamma$ 2; *Eco*RI for V $\gamma$ 3) for 1-hr digestion. Genomic DNA was purified from the digested nuclei and subjected to LM-PCR to detect restriction enzyme cleavage.

## Results

**A Transgenic Model to Test Role of V Gene Location in Developmentally Regulated V(D)J Recombination.** The  $\gamma$ B transgene consists of 39 kb of contiguous genomic DNA containing V $\gamma$ 2, V $\gamma$ 4, V $\gamma$ 3, J $\gamma$ 1, and C $\gamma$ 1 in their normal configuration (24). We previously used the identical backbone in the construction of  $\gamma$ B-Gn-Sw, the transgene used to demonstrate that promoter sequences regulate V gene usage in adult thymocytes (9) (Fig. 1). Starting with  $\gamma$ B, a 2.3-kb *Spe*I-*Eco*RI fragment containing V $\gamma$ 2 was reciprocally swapped with a 1.6-kb *Hind*III-*Eco*RI fragment containing V $\gamma$ 3, to generate the  $\gamma$ B-Gn-Sw construct (Fig. 1). The 5' endpoints of the exchanged fragments were identical to those used for the  $\gamma$ B-Pr-Sw. Therefore, the exchanged segments in the new  $\gamma$ B-Gn-Sw construct contain the identical promoter regions swapped in the promoter swap construct  $\gamma$ B-Pr-Sw and, in addition, the entire coding regions and 450–660 bp of DNA downstream of each RSS. In this way, the three transgenes can

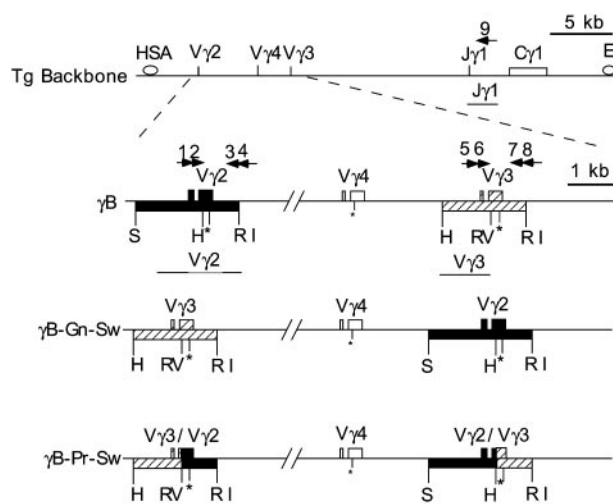


**Fig. 1.** Comparison of  $\gamma$ B,  $\gamma$ B-Gn-Sw, and  $\gamma$ B-Pr-Sw transgenes. The 5' DNase hypersensitive site A (HSA) and the 3' C $\gamma$ 1 enhancer, 3' E $\gamma$ 1 (E) are indicated. All transgenes have the same backbone. Differences are depicted in the expanded segments. The boxes above the line are the coding (V and leader) sequences. Boxes below the line are segments subjected to exchange. V $\gamma$ 2 sequences are in black and V $\gamma$ 3 are hatched. Asterisks indicate restriction enzyme sites introduced into the transgene. Restriction enzymes are as follows: S, *Spe*I; H, *Hind*III; R1, *Eco*RI; and RV, *Eco*RV. Arrows indicate positions and orientation of primers: 1, L2; 2, PSV $\gamma$ 2; 3, VG2I; 4, V2-3'a; 5, L3; 6, PSV $\gamma$ 3; 7, V3-3'b; 8, V3-3'a; and 9, J1. The labeled line segments indicate probes used in Southern blots.

be compared directly to distinguish the roles of the promoter sequences and gene location in V-J recombination. Each of the V $\gamma$  genes (V $\gamma$ 2, V $\gamma$ 4, and V $\gamma$ 3) in all three constructs contained in the coding region a restriction enzyme linker (*Nru*I, *Xho*I, and *Eco*RI, respectively) that allows the transgene and its transcripts to be readily distinguished from the corresponding endogenous  $\gamma$  genes and transcripts (9, 25). Furthermore, because the linkers introduce frameshift mutations that render the mutant proteins nonfunctional, the transgene is expected to confer no selective advantage or disadvantage to cells that express it.

Four  $\gamma$ B-Gn-Sw transgenic founders were generated and crossed with CBA mice. Three of the founders transmitted the transgene to their offspring, and one founder, a mosaic, did not transmit the transgene.

**V Gene Location Determines V $\gamma$  Rearrangement Pattern in DECJs.** V $\gamma$  gene rearrangements in DECJs, which are derived from early fetal thymocytes, were analyzed by semiquantitative PCR with a V $\gamma$ -specific primer and a common J $\gamma$ 1 primer (9). These primers amplify both transgene and endogenous rearrangements, which can be distinguished by electrophoresis after cleavage with restriction enzymes specific for the transgene (*Nru*I for V $\gamma$ 2 and *Eco*RI for V $\gamma$ 3). Compared with a typical  $\gamma$ B transgenic line, DECJs from all three  $\gamma$ B-Gn-Sw transgenic lines exhibited substantially elevated levels of transgene V $\gamma$ 2 rearrangements and substantially diminished levels of transgene V $\gamma$ 3 rearrangements (Fig. 2). Normalized to transgene copy number, V $\gamma$ 2 transgene rearrangements in  $\gamma$ B-Gn-Sw transgenics were elevated 5- to 10-fold, and V $\gamma$ 3 rearrangements were depressed 5- to 10-fold, in comparison with the mean values from several  $\gamma$ B transgenics. The average ratio of transgene V $\gamma$ 3 to V $\gamma$ 2 rearrangements in DEC cells is  $\approx$ 8:1 in  $\gamma$ B, 12:1 in  $\gamma$ B-Pr-Sw, and 6:1 in the endogenous locus (9). The corresponding ratio for the  $\gamma$ B-Gn-Sw transgenics is  $\approx$ 1:8, nearly a perfect reciprocal of the normal pattern. The mosaic  $\gamma$ B-Gn-Sw transgenic founder exhibited a similar reversal in the pattern of rearranged V $\gamma$ 3/V $\gamma$ 2

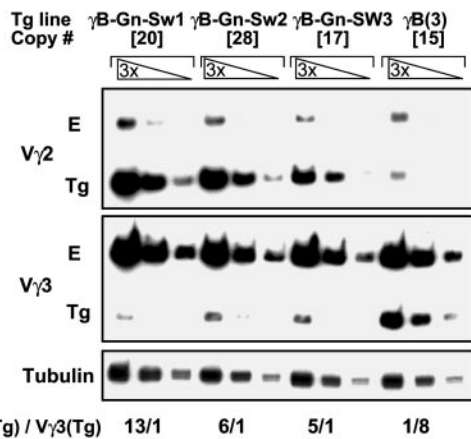


**Fig. 2.** Rearrangements in DEC cells of  $\gamma$ B-Gn-Sw and  $\gamma$ B transgenic mice. DEC cells from all three lines of  $\gamma$ B-Gn-Sw transgenic mice were compared with  $\gamma$ B (3) by semiquantitative PCR (9). Transgene copy number is indicated in brackets. Three-fold serial dilutions of DEC DNA samples were PCR amplified with the following primers (see Fig. 1): L2/J1 (for  $V\gamma 2$ ), L3/J1 (for  $V\gamma 3$ ), and 5'tubulin/3'tubulin (for Tub). PCR products were digested with *Nru*I (for  $V\gamma 2$ ) or *Eco*RI (for  $V\gamma 3$ ) to distinguish endogenous (E) from transgene (Tg) rearrangements. Semiquantitative PCR of tubulin was used to normalize the DNA samples. Ratios of the levels of  $V\gamma 2$  to  $V\gamma 3$  rearrangements of the transgene are displayed below each data set (see *Methods*).

genes except that the absolute  $V\gamma$  gene rearrangement levels were lower (data not shown). The reversed pattern of  $V\gamma$  rearrangement in DEC cells of the  $\gamma$ B-Gn-Sw transgene was also confirmed by Southern blot analysis (Fig. 6, which is published as supporting information on the PNAS web site). These results demonstrate that swapping the location of  $V\gamma 2$  and  $V\gamma 3$  genes completely reversed the rearrangement pattern of  $V\gamma 2/V\gamma 3$  genes in DEC cells. The consistency of this effect in different lines indicates that it is independent of transgene integration site.

**V Gene Location Determines  $V\gamma$  Rearrangement Pattern in Fetal but Not Adult Thymocytes.** Transgene rearrangements in E14 and E15 fetal thymi were also assessed. Compared with the  $\gamma$ B transgenics, transgene  $V\gamma 2$  rearrangements in  $\gamma$ B-Gn-Sw transgenics were elevated by an average of 4- to 5-fold whereas transgene  $V\gamma 3$  rearrangements were diminished by an average of 15- to 20-fold (Fig. 3*A* and Table 1). Consequently, the calculated ratio of rearranged  $V\gamma 2/V\gamma 3$  for the  $\gamma$ B-Gn-Sw transgene (6:1) is the near inverse of the corresponding ratio for the  $\gamma$ B transgene (1:10) or the endogenous TCR $\gamma$  genes (1:4) (9). The overall level of  $V\gamma 2$  plus  $V\gamma 3$  gene rearrangements per transgene copy in the  $\gamma$ B-Gn-Sw mice was only modestly lower (2- to 3-fold) than in  $\gamma$ B mice in the E15 fetal thymocytes (Table 1). A larger difference was observed in E14 fetal thymocytes, but this is at a stage where rearrangement is first initiated and the values for all of the transgenics were very low. These data suggest that, in the fetal thymus, the relative rearrangement levels of individual  $V\gamma$  genes are controlled by the locations of the V gene segments in the TCR  $C\gamma 1$  cluster, with little or no influence from the upstream promoter regions, the V coding regions, or the immediate downstream regions of the  $V\gamma$  genes including the RSSs.

In adult thymocytes,  $V\gamma 2$  rearrangements were more abundant than  $V\gamma 3$  rearrangements in both  $\gamma$ B-Gn-Sw and  $\gamma$ B transgenic thymocytes (Fig. 3*B*, Table 1, and Fig. 7, which is published as supporting information on the PNAS web site). The average ratio of  $V\gamma 2/V\gamma 3$  rearrangements in the three  $\gamma$ B-Gn-Sw transgenic lines was 3.7, comparable to 5.0 in the  $\gamma$ B transgenic mice (9), suggesting that  $V\gamma$  gene location has no or little effect on  $V\gamma$  gene rearrangement at the adult stage. Similar

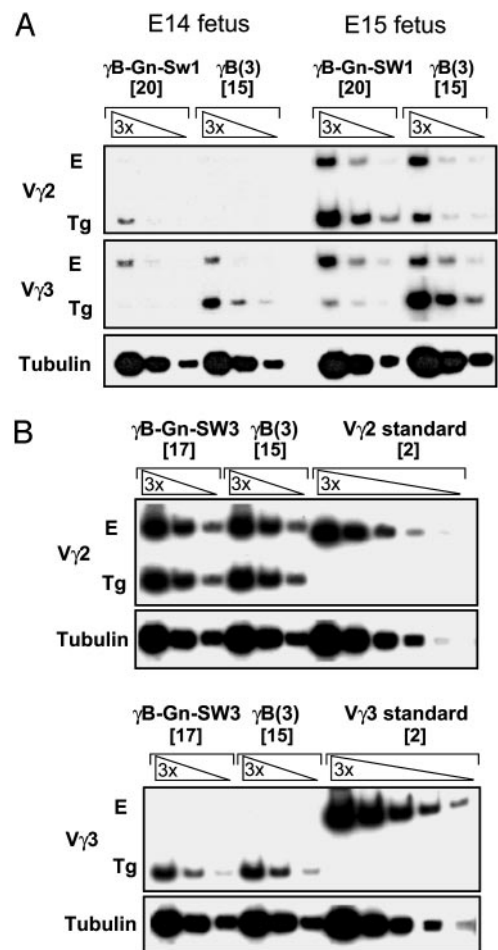


**Fig. 3.** Semiquantitative PCR of  $V\gamma 2$  and  $V\gamma 3$  rearrangements in early fetal and adult thymocytes of transgenic mice. (A) Comparison of  $V\gamma$  rearrangement in E14 thymus and E15 thymocytes. (B) Comparison of  $V\gamma$  rearrangement in adult  $CD4^+CD8^-$  thymocytes. The  $V\gamma 2$  standard is hybridoma DN2.3, which contains two copies of rearranged  $V\gamma 2$ . The  $V\gamma 3$  standard is the WRD.34 cell line, which contains two copies of rearranged  $V\gamma 3$ . See Fig. 2 legend for other details. Similar data for other lines are summarized in Table 1.

results were obtained in an analysis of adult splenic  $\gamma\delta$  T cells (data not shown).

**Extent of RSS Breaks Correlates with Location-Dependent  $V\gamma$  Gene Rearrangement Pattern.** To assess the possible steps of V-J recombination impacted by  $V\gamma$  gene location, we examined whether V gene location determined the extent of RAG-mediated DNA breaks at the RSSs flanking the  $V\gamma$  genes in the various transgenics. Breaks were assayed in thymocyte DNA by LM-PCR amplification of signal ends (19). By performing a limited number of PCR cycles, the experiment relied on the high number of transgene copies to distinguish breaks of transgene origin from those of endogenous origin. Under these conditions, no or little PCR products were detected in nontransgenic DNA from E15 fetal thymocytes (Fig. 4*A*). Significantly, in E15 fetal thymocytes, the  $\gamma$ B-Gn-Sw transgene contained >5-fold more  $V\gamma 2$  breaks and >5-fold fewer  $V\gamma 3$  breaks than the control  $\gamma$ B transgene, as determined by phosphorimaging and taking into account the difference in transgene copy number (Fig. 4*A Left*). These changes correlated well with the rearrangement pattern and suggested that the location of  $V\gamma$  genes in the transgene determined the RAG cleavage pattern. In adult thymocytes,  $V\gamma 2$  breaks were predominant, and  $V\gamma 3$  breaks were rare in both  $\gamma$ B

**Table 1. Rearrangement of V $\gamma$ 2 and V $\gamma$ 3 genes in thymocytes of the transgenic mice**

Line	Copy No.	E14 fetus			E15 fetus			Adult		
		V2*	V3*	V2/V3 <sup>†</sup>	V2	V3	V2/V3	V2	V3	V2/V3
$\gamma$ B-Gn-Sw1	20	0.00032	0.00012	2.7	0.0069	0.0012	5.8	0.130	0.032	4.1
$\gamma$ B-Gn-Sw2	28	0.00019	0.00002	11.6	0.0060	0.0013	4.9	0.069	0.032	3.0
$\gamma$ B-Gn-Sw3	17	ND	ND	ND	0.0073	0.0012	6.2	0.081	0.020	3.9
$\gamma$ B-Gn-Sw mean		0.00026	0.00007	7.1	0.0067	0.0012	5.6	0.093	0.028	3.7
$\gamma$ B-Pr-Sw mean <sup>‡</sup>		0.00003	0.00150	0.015	0.0018	0.0680	0.040	0.042	0.220	0.19
$\gamma$ B mean <sup>‡</sup>		0.00005	0.00325	0.024	0.0016	0.0190	0.095	0.120	0.049	2.47
End <sup>‡</sup>	2	0.00120	0.00330	0.364	0.0247	0.0930	0.266	0.380	0.015	25.33

ND, not done.

\*V2 and V3 refer to rearrangements of V $\gamma$ 2 and V $\gamma$ 3 per gene copy from PCR data.

<sup>†</sup>V2/V3 is ratio of rearranged V $\gamma$ 2 to rearranged V $\gamma$ 3 per gene copy.

<sup>‡</sup>Data for End (endogenous TCR $\gamma$ ),  $\gamma$ B, and  $\gamma$ B-Pr-Sw transgenes are from Baker (9).

and  $\gamma$ B-Gn-Sw transgenes, also consistent with the rearrangement pattern (Fig. 4A Right). In the  $\gamma$ B-Pr-Sw transgene, in contrast, V $\gamma$ 2 breaks in adult thymocytes were diminished and V $\gamma$ 3 breaks were sharply increased, consistent with the rearrangement pattern of this transgene.

**Germ-Line Transcription of V $\gamma$ 2/V $\gamma$ 3 Genes in  $\gamma$ B and  $\gamma$ B-Gn-Sw Transgenes.** Germ-line transcription of endogenous V $\gamma$  genes has been shown to correlate with the pattern of gene rearrangement (6). V $\gamma$  gene germ-line transcripts directed by the different transgenes were assayed by reverse transcription with primers 3' of the unrearranged V $\gamma$ 3 or V $\gamma$ 2 genes but within the exchanged segments in the  $\gamma$ B-Gn-Sw transgene. Serially diluted cDNA was amplified with a 5' primer in the V $\gamma$  coding region, and a downstream 3' primer internal to the primer was used for reverse transcription. The PCR products were cleaved with transgene-specific restriction enzymes to distinguish transgene-encoded and endogenous germ-line transcripts.

In E14 fetal thymocytes, transgene-derived germ-line V $\gamma$ 2 transcripts were slightly more abundant in the  $\gamma$ B-Gn-Sw sample than in the  $\gamma$ B sample, and V $\gamma$ 3 germ-line transcripts slightly less abundant (Fig. 4B Left). When data from different lines were normalized for transgene copy number and averaged, these differences were small, averaging 2.4-fold for V $\gamma$ 2 and 1.5-fold for V $\gamma$ 3. Although the increase in V $\gamma$ 2 germ-line transcription did not grossly differ in magnitude from the increase in the level of V $\gamma$ 2 rearrangement (4- to 5-fold), the minor decrease in V $\gamma$ 3 germ-line transcription contrasted with the much larger decrease in V $\gamma$ 3 rearrangements (15- to 20-fold) and RSS breaks evident with the  $\gamma$ B-Gn-Sw transgene at the fetal stage. Thus, the reduced rearrangement of V $\gamma$ 3 was not accompanied by a corresponding decrease in germ-line transcription.

There was little difference in germ-line transcription in adult thymocytes between the  $\gamma$ B and  $\gamma$ B-Gn-Sw transgenes, as expected based on their similar rearrangement pattern (Fig. 4B Right). As a comparison, we examined germ-line transcription of the  $\gamma$ B-Pr-Sw transgene, which exhibits a reciprocal rearrangement pattern in adult thymocytes compared with  $\gamma$ B. The analysis revealed that V $\gamma$ 3 germ-line transcripts per transgene copy were increased by an average of 5-fold compared with  $\gamma$ B whereas V $\gamma$ 2 transcripts were decreased by an average of 3-fold, consistent with the expected effects of promoter regions (Fig. 4C). The magnitude of these differences in germ-line transcription correlated well with the changes in rearrangement observed with this transgene (9). We conclude that, whereas the promoter-dependent adult pattern of transgene rearrangement correlates well with changes in germ-line transcription, the location-dependent fetal pattern of transgene rearrangement does not.

**Restriction Enzyme Accessibility of V $\gamma$  Genes in  $\gamma$ B and  $\gamma$ B-Gn-Sw Transgenes.** The changed rearrangement pattern as a result of relocalization of the V $\gamma$  genes in the transgene could be due to changes in the "accessibility" of the local chromatin to the recombinase. V $\gamma$  gene accessibility was examined by assaying the susceptibility of V $\gamma$  genes in thymocyte nuclei to restriction enzyme cleavage, by using LM-PCR. Preliminary analysis showed that accessibility of the V $\gamma$ 2 and V $\gamma$ 3 genes to restriction enzymes was substantially lower in irrelevant perfused adult liver cells than in adult thymocytes (data not shown). In E15 fetal thymocytes, an Asp-718 site in the V $\gamma$ 2 coding region (Fig. 5A) was slightly less accessible in  $\gamma$ B-Gn-Sw transgenics, despite the increase in rearrangement (Fig. 5B). The PCR products were essentially all cleaved by *Nru*I, specific for a site unique to the transgenes (Fig. 5B). Also in E15 fetal thymocytes, a transgene-specific *Eco*RI site in the coding region of the V $\gamma$ 3 gene near the RSS (Fig. 5A) was equally accessible, or only slightly less accessible (depending on the experiment) in the  $\gamma$ B-Gn-Sw transgene compared with the  $\gamma$ B transgene (Fig. 5C). A minor reduction in accessibility of V $\gamma$ 3 gene in the  $\gamma$ B-Gn-Sw transgene was observed at another restriction enzyme site, *Apa*LI (data not shown). An analysis of adult thymocyte nuclei revealed a pattern very similar to that of fetal thymocytes: the two transgenes showed similar levels of accessibility of the Asp-718 site in V $\gamma$ 2, and the  $\gamma$ B-Gn-Sw transgene exhibited a slight reduction in accessibility of the *Eco*RI or *Apa*LI sites in the V $\gamma$ 3 gene (Fig. 5D and E and data not shown). Thus, the strongly altered pattern of rearrangement and RSS breakage due to relocation of the V $\gamma$  genes in fetal thymocytes was not accompanied by similar alterations in V $\gamma$  gene accessibility. These findings suggest that V gene location determines the rearrangement pattern predominantly by a mechanism independent of accessibility.

## Discussion

The results reported here demonstrate that the locations of V $\gamma$ 2 and V $\gamma$ 3 genes in a TCR $\gamma$  transgene determine the pattern of gene rearrangement in fetal thymocytes and DEC. The results represent an experimental demonstration that the relative location of V gene segments is a direct determinant of preferential V gene recombination. It is possible that a similar principle contributes to developmentally regulated V gene segment rearrangement in the IgH, TCR $\delta$ , and possibly other receptor gene families. Previous studies have shown that RSSs (26) and promoters (9) can differentially regulate gene segment rearrangement during development, but the present results argue that these elements do not play a primary role in determining the fetal/DEC pattern of rearrangement.

V gene location did not affect the rearrangement pattern in the adult thymus. Therefore, V $\gamma$  gene rearrangement at the adult

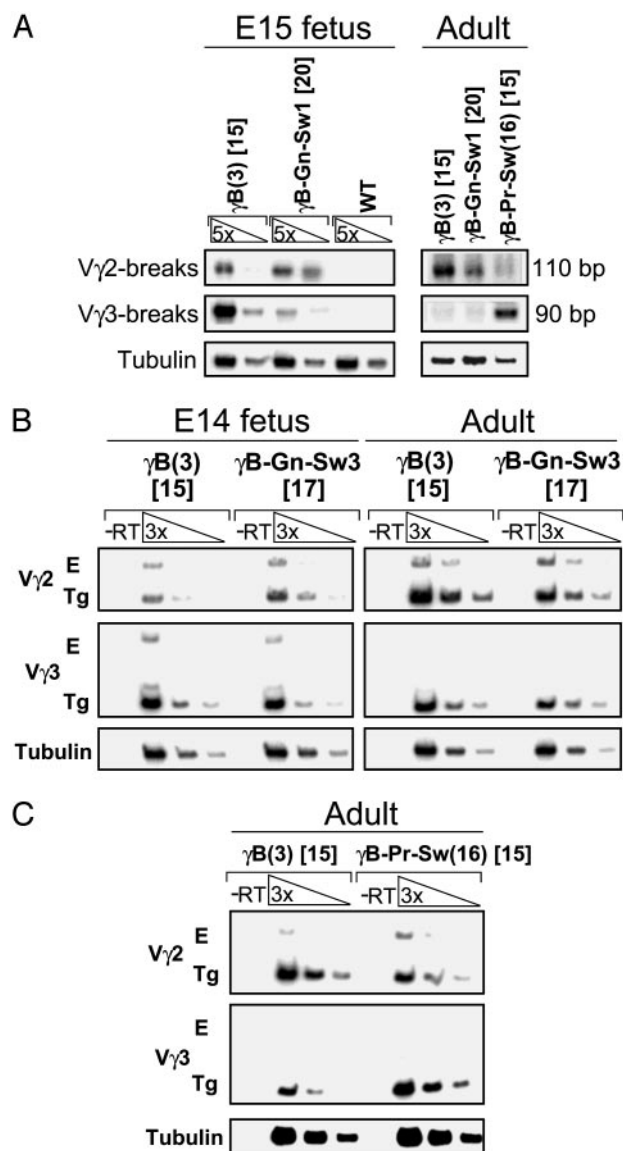


**Fig. 4.** RSS breaks and germ-line transcription of V $\gamma$ 2 and V $\gamma$ 3 genes in the transgenes. (A) Comparison of RSS breaks flanking V $\gamma$ 2 and V $\gamma$ 3 in the transgenes. Samples were serially diluted 5-fold (for E15 fetal samples). Semiquantitative PCR for tubulin was used as a loading control. (B) V $\gamma$ 2 and V $\gamma$ 3 germ-line transcripts emanating from transgenes in fetal and adult thymocytes. Shown is semiquantitative RT-PCR analysis of germ-line transcripts in total RNAs from adult CD4<sup>+</sup> CD8<sup>-</sup> thymocytes and E14 fetal thymus of  $\gamma$ B and  $\gamma$ B-Gn-Sw transgenic mice. Primers for reverse transcription (RT) included oligo(dT) (for the tubulin control), V2-3'a (for V $\gamma$ 2), or V3-3'b (for V $\gamma$ 3) (see Fig. 1). RT products were then 3-fold serially diluted and subjected to the semiquantitative PCR. Either 5'tubulin/3'tubulin primer set (for Tub) or L2/VG21 primer set (for V $\gamma$ 2), or PSV $\gamma$ 3/V3-3'b primer set (for V $\gamma$ 3) was used for PCR of corresponding RT products. V $\gamma$ 2 and V $\gamma$ 3 PCR products were digested with *Nru*I (for V $\gamma$ 2) or *Eco*RI (for V $\gamma$ 3) before gel fractionation. RNA samples without RT were also directly subjected to the semiquantitative PCR to confirm the absence of DNA contamination in the samples. (C) Germ-line transcripts of  $\gamma$ B and  $\gamma$ B-Pr-Sw transgenes in adult CD4<sup>+</sup> CD8<sup>-</sup> thymocytes. The PSV $\gamma$ 2/VG21 primer set was used for V $\gamma$ 2 PCR. All others were as in B.

stage is largely dependent on promoters, as previously suggested (9). The separate regulation of the fetal and adult patterns of rearrangement was also suggested by the finding that E2A deficiency reverses the adult but not the fetal pattern of rearrangement (27). Taken together, the results indicate that the "developmental switch" in V $\gamma$  gene usage is imposed by at least

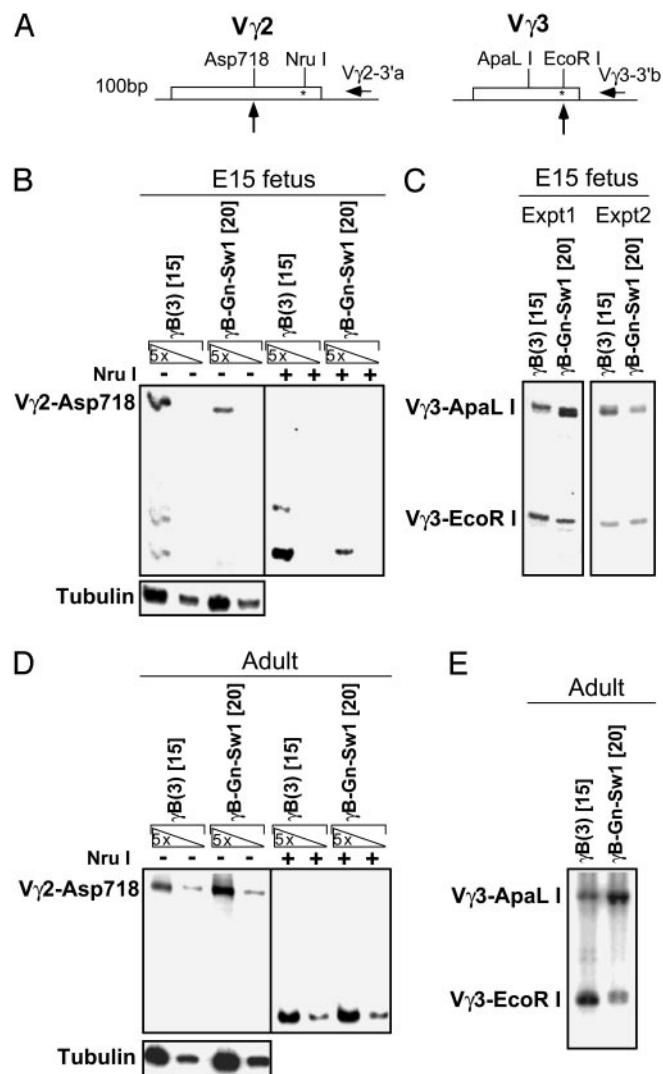


**Fig. 5.** Restriction enzyme accessibility of V $\gamma$ 2 and V $\gamma$ 3 genes in the transgenes. (A) Restriction enzyme sites in V $\gamma$ 2 and V $\gamma$ 3 genes used in the accessibility assays. The *Nru*I and *Eco*RI sites indicated with asterisks are transgene-specific sites. Vertical arrows indicate the restriction sites probed in these analyses. Nuclei of E15 fetal thymocytes (B and C) or adult CD4<sup>+</sup> CD8<sup>-</sup> thymocytes (D and E) were treated with restriction enzymes to detect the accessibility of the V $\gamma$ 2 (Asp-718) or V $\gamma$ 3 (*Eco*RI) genes. After DNA extraction, cleavage was assayed by radioactive LM-PCR. (B and D) The accessibility of the Asp-718 site in the V $\gamma$ 2 gene. Samples were serially diluted 5-fold. Semiquantitative PCR for the tubulin gene was used as a loading control. A portion of each PCR product was digested with *Nru*I before gel fractionation to confirm its origin from the transgene. (C and E) The accessibility of the *Eco*RI site in V $\gamma$ 3 gene was determined. In this assay, the DNA was digested with a second restriction enzyme, ApaI (located 5' of the *Eco*RI site) after DNA extraction but before LM-PCR. Therefore, the ApaI PCR product corresponds to DNA that was uncleaved by *Eco*RI and serves as an internal reference. In C, two experiments are shown for comparison.

two mechanisms, one sensitive to gene location and the other dependent on differential V-promoter activity.

In comparing the transgenes, the RSS of the most proximal V $\gamma$  gene was more frequently broken in chromatin of fetal thymocytes, suggesting that location of the gene determines its susceptibility to RAG-mediated cleavage. It was notable, however, that accessibility and germ-line transcription of V $\gamma$ 2 and V $\gamma$ 3 genes in fetal thymocytes were not substantially altered between the  $\gamma$ B and  $\gamma$ B-Gn-Sw transgenics. These results suggest that

both V $\gamma$ 2 and V $\gamma$ 3 genes are substantially accessible in early fetal thymocytes of both transgenes, consistent with a report that V $\gamma$ 2 and V $\gamma$ 3 in the endogenous locus exhibited similar levels of histone hyperacetylation at the fetal stage (17). Although both genes are apparently accessible at the early fetal stage, the downstream gene undergoes preferential RSS breakage and recombination.

One explanation of the location dependence of rearrangement in the fetal stage is that the locus is separated into discrete domains under independent regulation, and the swap of the V $\gamma$  genes places each into the domain of the other. For example, it has been proposed that D<sub>H</sub>-J<sub>H</sub> joining activates the rearrangement of a domain containing 3' V<sub>H</sub> genes in the IgH locus, but that signaling by IL-7 or the v-abl tyrosine kinase is necessary for rearrangement of V<sub>H</sub> genes in upstream domains (28, 29). If V $\gamma$  genes are organized in domains, however, their regulation is not well correlated with accessibility or germ-line transcription at the fetal stage.

Another possibility is that proximity to J $\gamma$ 1 itself may determine the V $\gamma$  gene rearrangement frequency at the fetal stage. Proximity to J $\gamma$ 1 may increase the likelihood of random interactions between the two participating RSSs, or there may be a processive component to the recombination process. Preferential pairing of the most proximal V $\gamma$  RSS with the J $\gamma$ 1 RSS could also account for increased levels of breaks observed at the RSS of the proximal V $\gamma$  gene because cleavage occurs preferentially at paired RSSs.

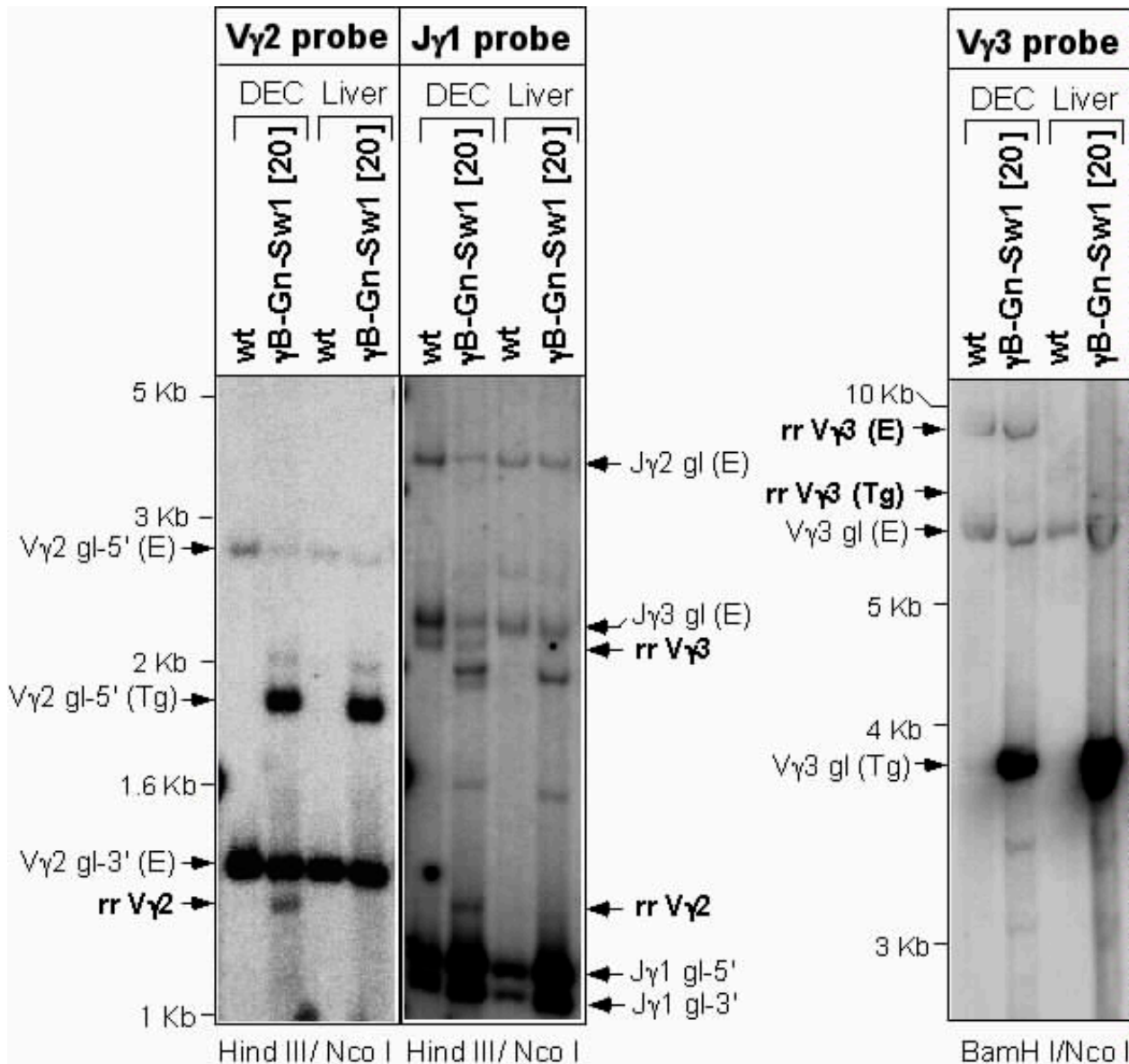
It is also possible that the key determinant of rearrangement at the early fetal stage is proximity of the V $\gamma$  gene to a downstream transcriptional regulatory element, reminiscent of a study showing that proximity of globin genes to the  $\beta$  globin locus

control region determines the extent of globin gene transcription early in erythropoiesis (30). We disfavor this explanation for our results because we observed that V $\gamma$  gene location is not a primary determinant of germ-line transcription levels or accessibility, both properties that would arguably be associated with enhancer activity. Furthermore, we showed that the fetal pattern of rearrangement was normal on a chromosome from which the obvious candidate element in the downstream region, 3' E<sub>C</sub> $\gamma$ 1, was deleted (20). It remains possible that proximity to another, undefined, downstream element determines the fetal rearrangement pattern, but by a mechanism other than regulating locus accessibility.

At the adult stage, V $\gamma$ 3 rearrangement is repressed, and V $\gamma$ 2 rearrangement predominates. A strong reduction in V $\gamma$ 3 germ-line transcription and histone hyperacetylation accompanies this switch (6, 17). When the V $\gamma$ 2 and V $\gamma$ 3 promoters were swapped, V $\gamma$ 2 rearrangement decreased and V $\gamma$ 3 rearrangements increased (9). As shown here, the changes in rearrangement were mirrored by comparable changes in germ-line transcription. Thus, promoter-dependent repression of V $\gamma$ 3 rearrangement is likely accompanied by reduced accessibility and transcription of V $\gamma$ 3 and may also involve increased accessibility of V $\gamma$ 2. The picture that begins to emerge is one where the two genes are both relatively accessible in the early stages, with an advantage to the more proximal gene (normally V $\gamma$ 3), followed by the late stage where the V $\gamma$ 3 gene is repressed and/or V $\gamma$ 2 is activated, leading to a strong preference for V $\gamma$ 2 rearrangement.

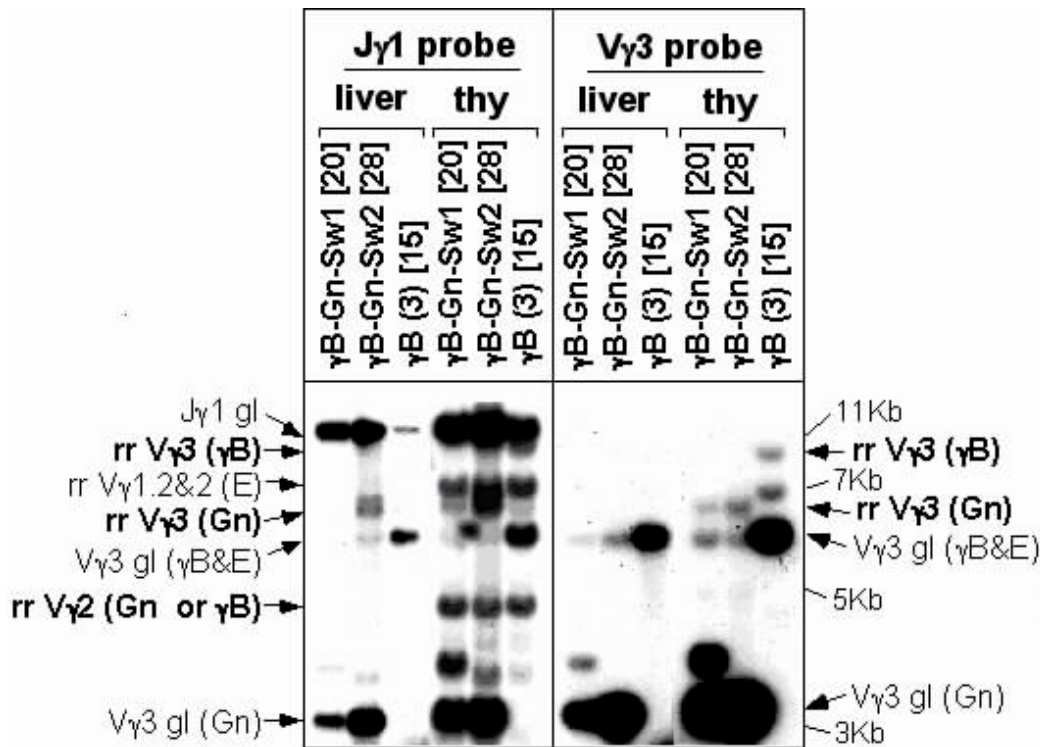
We thank Mark Schlissel for valuable advice and Dawn Tanamachi for help in construction of the  $\gamma$ B-Gn-Sw transgene. This work was supported by Grant R01-A131650 from the National Institutes of Health (to D.H.R.).

1. Raulet, D. H. (1989) *Annu. Rev. Immunol.* **7**, 175–207.
2. Elliott, J. F., Rock, E. P., Patten, P. A., Davis, M. M. & Chien, Y.-H. (1988) *Nature* **331**, 627–631.
3. Yancopoulos, G. D., Desiderio, S. V., Paskind, M., Kearney, J. F., Baltimore, D. & Alt, F. W. (1984) *Nature* **311**, 727–733.
4. Malynn, B. A., Yancopoulos, G. D., Barth, J. E., Bona, C. A. & Alt, F. W. (1990) *J. Exp. Med.* **171**, 843–859.
5. Yancopoulos, G. D. & Alt, F. W. (1985) *Cell* **40**, 271–281.
6. Goldman, J., Spencer, D. & Raulet, D. (1993) *J. Exp. Med.* **177**, 729–739.
7. Stanhope-Baker, P., Hudson, K. M., Shaffer, A. L., Constantinescu, A. & Schlissel, M. S. (1996) *Cell* **85**, 887–897.
8. Sleckman, B. P., Bassing, C. H., Bardon, C. G., Okada, A., Khor, B., Bories, J. C., Monroe, R. & Alt, F. W. (1998) *Immunol. Rev.* **165**, 121–130.
9. Baker, J. E., Cado, D. & Raulet, D. H. (1998) *Immunity* **9**, 159–168.
10. Yancopoulos, G. D., Malynn, B. A. & Alt, F. W. (1988) *J. Exp. Med.* **168**, 417–435.
11. Garman, R. D., Doherty, P. J. & Raulet, D. H. (1986) *Cell* **45**, 733–742.
12. Heilig, J. S. & Tonegawa, S. (1986) *Nature* **322**, 836–840.
13. Chien, Y.-H., Iwashima, M., Wettstein, D. A., Kaplan, K. B., Elliott, J. F., Born, W. & Davis, M. M. (1987) *Nature* **330**, 722–727.
14. Allison, J. P. & Havran, W. L. (1991) *Annu. Rev. Immunol.* **9**, 679–705.
15. Itohara, S., Mombaerts, P., Lafaille, J., Iacomini, J., Nelson, A., Clarke, A. R., Hooper, M. L., Farr, A. & Tonegawa, S. (1993) *Cell* **72**, 337–348.
16. Raulet, D., Spencer, D., Hsiang, Y.-H., Goldman, J., Bix, M., Liao, N.-S., Zijlstra, M., Jaenisch, R. & Correa, I. (1991) *Immunol. Rev.* **120**, 185–204.
17. Agata, Y., Katakai, T., Ye, S. K., Sugai, M., Gonda, H., Honjo, T., Ikuta, K. & Shimizu, A. (2001) *J. Exp. Med.* **193**, 873–879.
18. Asarnow, D. M., Goodman, T., LeFrancois, L. & Allison, J. P. (1989) *Nature* **341**, 60–62.
19. Schlissel, M., Constantinescu, A., Morrow, T., Baxter, M. & Peng, A. (1993) *Genes Dev.* **7**, 2520–2532.
20. Xiong, N., Kang, C. H. & Raulet, D. H. (2002) *Immunity* **16**, 453–463.
21. Sullivan, S., Bergstresser, P., Tigelaar, R. & Streilein, J. W. (1985) *J. Invest. Dermatol.* **84**, 491–495.
22. Ausubel, F., Brent, R., Kingston, R., Moore, D., Seidman, J., Smith, J. & Struhl, K. (1991) *Current Protocols in Molecular Biology* (Greene, New York).
23. Weinmann, A. S., Plevy, S. E. & Smale, S. T. (1999) *Immunity* **11**, 665–675.
24. Baker, J. E., Kang, J., Xiong, N., Chen, T., Cado, D. & Raulet, D. H. (1999) *J. Exp. Med.* **190**, 669–679.
25. Asarnow, D. M., Cado, D. & Raulet, D. H. (1993) *Nature* **362**, 158–160.
26. Bassing, C. H., Alt, F. W., Hughes, M. M., D'Auteuil, M., Wehrly, T. D., Woodman, B. B., Gärtner, F., White, J. M., Davidson, L. & Sleckman, B. P. (2000) *Nature* **405**, 583–586.
27. Bain, G., Romanow, W. J., Albers, K., Havran, W. L. & Murre, C. (1999) *J. Exp. Med.* **189**, 289–300.
28. Chowdhury, D. & Sen, R. (2001) *EMBO J.* **20**, 6394–6403.
29. Corcoran, A. E., Riddell, A., Krooshoop, D. & Venkitaraman, A. R. (1998) *Nature* **391**, 904–907.
30. Tanimoto, K., Liu, Q., Bungert, J. & Engel, J. D. (1999) *Nature* **398**, 344–348.

[Full Text of this Article](#)

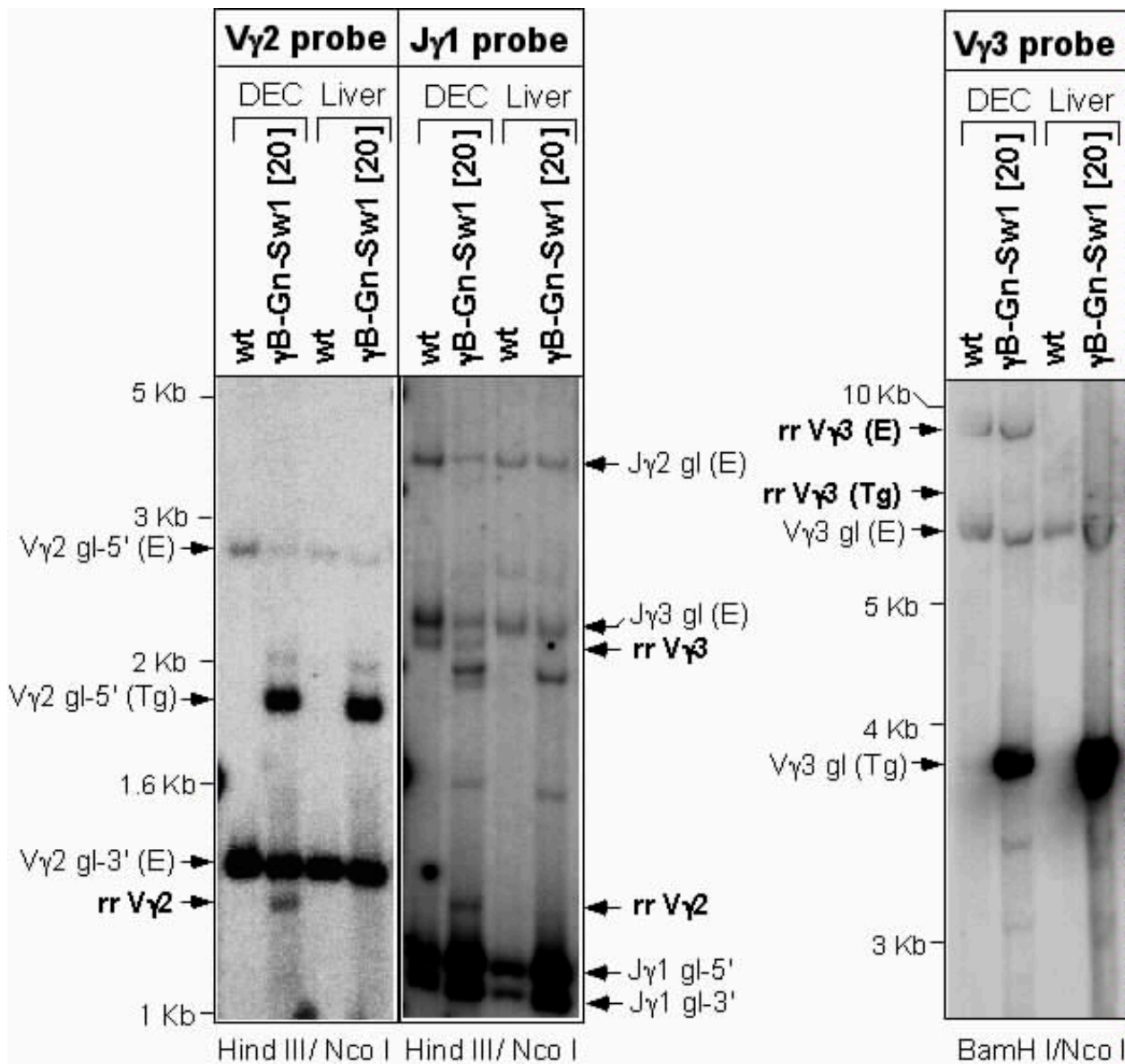
**Fig. 6.** Southern blot analysis comparing V $\gamma$ 2 and V $\gamma$ 3 rearrangements in dendritic epidermal T cells (DECs) from  $\gamma$  B-Gn-Sw1 transgenic and nontransgenic wild-type mice. V $\gamma$ 2, J $\gamma$ 1, and V $\gamma$ 3 probes used in the Southern blot analysis were a 2-kb *Xba*I-*Eco*RI fragment, a 3-kb *Eco*RV fragment, and a 0.8-kb *Hind*III-*Eco*RV fragment, as depicted in Fig. 1. The cultured DEC cell preparation contained at least 50%



[Full Text of this Article](#)


**Fig. 7.** Southern blot analysis of rearrangement of  $V\gamma 2$  and  $V\gamma 3$  genes in adult thymocytes of  $\gamma B$ -Gn-Sw and  $\gamma B$  transgenic mice. Genomic DNA was digested with *Bam*HI, *Nco*I, and *Nru*I. The blot was first probed with a  $V\gamma 3$  probe and rehybridized with the  $J\gamma 1$  probe. Identities of the bands, where known, are indicated. Note that a germ-line  $J\gamma 1$ -hybridizing fragment (i.e., present in liver DNA) unique to the  $\gamma B$ -Gn-Sw2 transgenic line happens to comigrate with the rearranged  $V\gamma 3$  band in the thymocyte sample. rr, rearranged; gl, germ-line; Gn,  $\gamma B$ -Gn-Sw transgene;  $\gamma B$ ,  $\gamma B$  transgene; E, endogenous. Hybridization with a  $J\gamma 1$  probe revealed that  $V\gamma 2$  rearrangements were more abundant than  $V\gamma 3$  rearrangements in both  $\gamma B$ -Gn-Sw and  $\gamma B$  transgenic thymocytes.

[Full Text of this Article](#)

[Full Text of this Article](#)

**Fig. 6.** Southern blot analysis comparing  $V\gamma 2$  and  $V\gamma 3$  rearrangements in dendritic epidermal T cells (DECs) from  $\gamma B$ -Gn-Sw1 transgenic and nontransgenic wild-type mice.  $V\gamma 2$ ,  $J\gamma 1$ , and  $V\gamma 3$  probes used in the Southern blot analysis were a 2-kb *XbaI-EcoRI* fragment, a 3-kb *EcoRV* fragment, and a 0.8-kb *HindIII-EcoRV* fragment, as depicted in Fig. 1. The cultured DEC cell preparation contained at least 50%

V $\gamma$ 3<sup>+</sup> DEC. Liver DNA was employed as a nonrearranging tissue. DNAs of DEC or livers were digested with indicated enzymes and hybridized with the indicated probes, which correspond to the fragments depicted in Fig. 1. Several bands are present in the J $\gamma$ 1 blot, due to cross-hybridization of the probe with J $\gamma$ 2 and J $\gamma$ 3. The identity of the bands, where known, is indicated. The V $\gamma$ 2 and J $\gamma$ 1 probes each hybridize with two germ-line fragments (5' and 3') due to the presence of *Hind*III sites in both segments. wt, wild-type; gl, germ-line; rr, rearranged; Tg, transgene; E, endogenous. The J $\gamma$ 1 blot allows V $\gamma$ 2 and V $\gamma$ 3 rearrangements to be directly compared in the same sample where V $\gamma$ 2 rearrangements were clearly evident in  $\gamma$ B-Gn-Sw transgenics. Endogenous V $\gamma$ 2 rearrangements comigrate with transgene rearrangements, but, because they are undetectable in nontransgenic DEC, the V $\gamma$ 2 rearrangements are therefore derived from the transgene. Endogenous V $\gamma$ 3 rearrangements are abundant in DEC and comigrate with transgene V $\gamma$ 3 rearrangements in the J $\gamma$ 1 blot. They can be distinguished in the V $\gamma$ 3 blot. Transgene V $\gamma$ 3 rearrangements (6.8-kb band) were just barely detectable in this analysis whereas endogenous V $\gamma$ 3 rearrangements (9.6-kb band) were abundant as expected. PhosphorImager analysis of the filter probed with J $\gamma$ 1 revealed that V $\gamma$ 2 rearrangements were 3-fold more abundant than V $\gamma$ 3 rearrangements in DEC cell DNA from the transgenics. Because approximately 20% of the V $\gamma$ 3 rearrangements in this analysis were of transgene origin (V $\gamma$ 3 blot), the ratio of transgene V $\gamma$ 2 to V $\gamma$ 3 rearrangements is approximately 15.

[Full Text of this Article](#)

[HOME](#) [HELP](#) [FEEDBACK](#) [SUBSCRIPTIONS](#) [ARCHIVE](#) [SEARCH](#)

[Copyright © by the National Academy of Sciences](#)

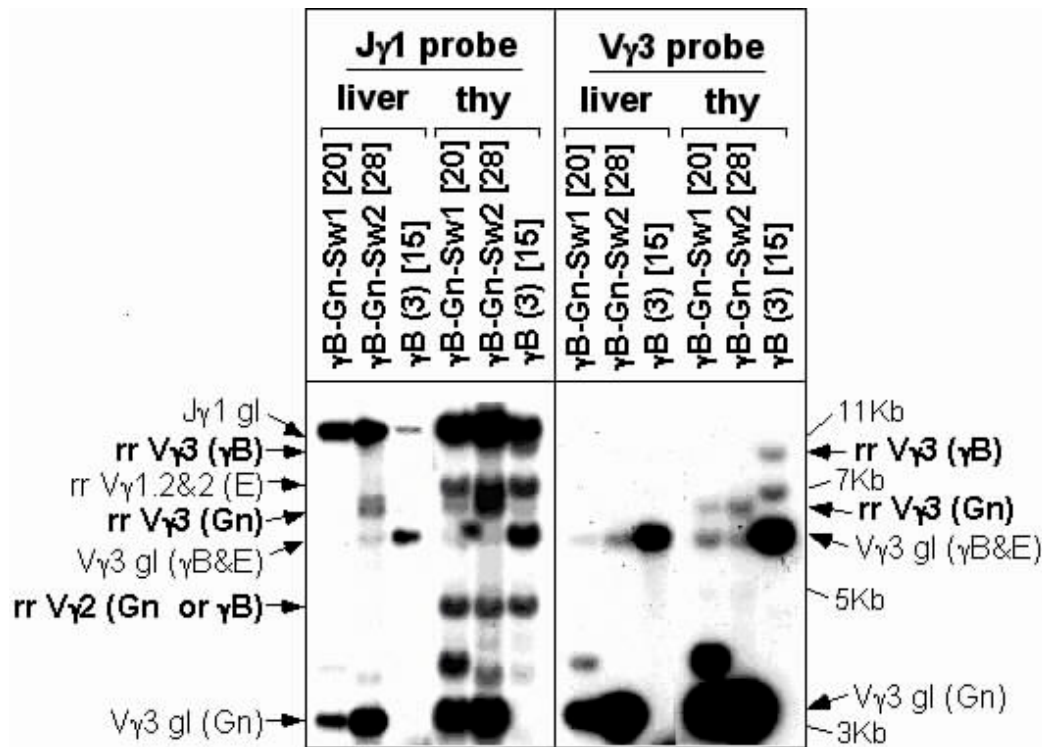


**Fig. 7.** Southern blot analysis of rearrangement of  $V\gamma 2$  and  $V\gamma 3$  genes in adult thymocytes of  $\gamma B$ -Gn-Sw and  $\gamma B$  transgenic mice. Genomic DNA was digested with *Bam*HI, *Nco*I, and *Nru*I. The blot was first probed with a  $V\gamma 3$  probe and rehybridized with the  $J\gamma 1$  probe. Identities of the bands, where known, are indicated. Note that a germ-line  $J\gamma 1$ -hybridizing fragment (i.e., present in liver DNA) unique to the  $\gamma B$ -Gn-Sw2 transgenic line happens to comigrate with the rearranged  $V\gamma 3$  band in the thymocyte sample. rr, rearranged; gl, germ-line; Gn,  $\gamma B$ -Gn-Sw transgene;  $\gamma B$ ,  $\gamma B$  transgene; E, endogenous. Hybridization with a  $J\gamma 1$  probe revealed that  $V\gamma 2$  rearrangements were more abundant than  $V\gamma 3$  rearrangements in both  $\gamma B$ -Gn-Sw and  $\gamma B$  transgenic thymocytes.